UNIVERSITY OF CALIFORNIA, SAN DIEGO

The Role of Interleukin-33 in the Progression of Pulmonary Arterial Hypertension Through an ST2/MyD88 Pathway

A Thesis submitted in partial satisfaction of the requirements
for the degree Master of Science

in

Biology

by

Alma Karla Gutierrez

Committee in Charge:

Mark Fuster, Chair
Kathleen French, Co-Chair
Ellen Breen
Elina Zuniga

2018

The Thesis of Alma Karla Gutierrez is approved, and is acceptable in quality and form for publication on microfilm and electronically:

Co-Chair

Chair

University of California, San Diego

2018

DEDICATION

I dedicate this thesis to my husband, Michael, for his unconditional love and support throughout all these years. It has been a long and arduous journey, but it was made easier with you by my side – always believing in me, and always there to encourage me. I would also like to dedicate this thesis to my parents for all the sacrifices they made to give me the opportunity to have a great education and a better life. To Dad, may you rest in peace, thank you for everything. None of this would have been possible without you always there by our side. To my entire family, thank you for your love, support, encouragement and understanding throughout this long endeavor.

TABLE OF CONTENTS

LIST OF FIGURES

LIST OF TABLES

LIST OF ABRREVIATIONS

PAH = pulmonary arterial hypertension

PVR = pulmonary vascular resistance

RVP = right ventricular pressures

O_2 = oxygen

S.C. = subcutaneous

SU5416 = Sugen 5416, a potent and selective synthetic inhibitor of the VEGF receptor tyrosine kinase

SuHx = Sugen 5416/Hypoxia

DMSO/RA = dimethyl sulfoxide/room air

IL-33 = interleukin-33

C57Bl/6J = C57 Black 6J

WT = wild-type

ST2 = suppressor of tumorigenicity 2

ST2 -/- = suppressor of tumorigenicity 2 knockout

sST2 = a soluble form of the receptor, ST2

ST2L = the transmembrane form of ST2, long

MyD88 = myeloid differentiation primary response gene 88

MyD88 -/- = myeloid differentiation primary response gene 88 knockout

VEGF = vascular endothelial growth factor

I.P. = intraperitoneal

Cre = Cre recombinase

BrdU = 5-bromo-2’deoxyuridine

ACKNOWLEDGMENTS

I would like to take this opportunity to thank Dr. Ellen Breen for allowing me to be a part of her lab. Your support, time, guidance, and most importantly, patience as my advisor for this project has made this all possible. Thank you for teaching me so many valuable laboratory techniques and for helping me edit my writing numerous times. I could not have done this without you.

I would like to thank Dr. Mark Fuster for agreeing to join this project as my mentor after Dr. Bigby's passing. You made it possible for me to continue to pursue my education and desire to contribute to the advancement of research in medicine, and for that, I cannot thank you enough. Thank you for giving me support, advice, new ideas and time, all of which contributed to the development of this project.

I would like to thank my committee members, Dr. Kathleen French and Dr. Elina Zuniga, for taking the time out of your busy schedules to be here and be a part of this project, and for helping me see it to its completion.

I would like to thank Scott Johns. Your help and guidance have not only contributed to the development of Figure 4, but to many other aspects of this project through your vast knowledge and experience in science and research.

I would like to thank Daniel Cannon. Having you as part of this extended project made this experience that much more meaningful. Your words of encouragement and positivity along with your extensive knowledge and background in all aspects of science were all an excellent source of motivation and made this journey quite special.

I would like to acknowledge the late Dr. Timothy Bigby who sadly passed away on April 4, 2016. I would like to thank Dr. Bigby for allowing me to join his lab, for being my mentor, for his support, guidance, patience, and sincerity. Dr. Bigby was there for us even through his illness, and he continued to be there for us after his passing by continuing to fund our projects. His dedication to medicine and the advancement in research have been a continuing inspiration for me throughout this journey.

Figures 1 and 2 are reprints of material presented at Center for Physiological Genomics of Low Oxygen Summit 2017 (Gutierrez 2017). A special thanks to Andrew Lerner and Colin Tsui for getting this project started and teaching me the techniques necessary to obtain our measurements and maintain the mouse colonies all of which were integral to our study.

The work presented in Figure 3 and part of Tables 1 and 2 have been submitted as an abstract to be presented at American Thoracic Society in 2018 (Gutierrez 2018). A special thank you to Yiming Kang, Eva Alberch Campubrí, and Judit Platero Diago for their help with the processing of the tissues and their companionship.

Slides were scanned at the UCSD School of Medicine Microscopy Core, which is supported by the UCSD Neuroscience Microscopy Shared Facility Grant (P30 NS047101).

The Introduction, Materials and Methods, Results and Discussion sections of this thesis will be prepared, in part, for submission for publication of the material. The thesis author was the primary investigator and author of this material.

Support: VA Department of Veterans Affairs and UCSD Academic Senate

ABSTRACT OF THE THESIS

The Role of Interleukin-33 in the Progression of Pulmonary Arterial Hypertension Through an ST2/MyD88 Pathway

by

Alma Karla Gutierrez

Master of Science in Biology

University of California, San Diego, 2018

Mark Fuster, Chair

Kathleen French, Co-Chair

Pulmonary arterial hypertension (PAH) is a multifactorial disorder characterized by elevated right ventricle pressures (RVP) and pulmonary vascular resistance (PVR) thought to result from pulmonary vascular remodeling. Currently, there is no cure for PAH, but inflammatory mechanisms have been implicated in playing a role. Previously, members of our

group measured elevated levels of interleukin-33 (IL-33) in Group 1 PAH patient serum. This alarmin, “danger” signal, is expressed by endothelial cells and its signaling can either repair the endothelial layer or, if the danger signals persist, contribute to uncontrolled proliferation. Thus, we hypothesized that pulmonary vascular remodeling in PAH is regulated by an IL-33-dependent pathway. To test this hypothesis, PAH was induced in adult C57BL/6J (wild-type, WT) mice, IL-33 receptor gene-ablated mice (ST2 -/-), in mice with a gene deletion of the upstream adaptor, MyD88 (MyD88 -/-), and in a strain with a conditional, endothelial-specific IL-33 gene-targeted inactivation using *IL33* floxed and Tek-Cre transgenes [Tek-Cre (+/-)::$IL33^{fl/fl}$]. Body weight, RVP, pulmonary vascular remodeling and endothelial cell proliferation were evaluated. PAH was induced using 10% hypoxia and weekly injections of the VEGF receptor antagonist, SU5416 (20 mg/kg) for three weeks (SuHx). The control condition was vehicle and room air, (DMSO/RA). RVP were measured by right heart catheterization in anesthetized mice. Pulmonary vascular wall thickness was morphometrically analyzed from paraffin-embedded H&E sections. Endothelial cell proliferation was analyzed by flow cytometry. Following SuHx conditions: all mice lost weight, except for MyD88 -/- mice, and RVP were increased in WT and Tek-Cre::$IL33^{fl/fl}$ mice, but attenuated in ST2 -/-, and MyD88 -/- mice. Pulmonary vascular wall thickening increased in WT-SuHx males and Tek-Cre::IL-$33^{fl/fl}$ males, but not in SuHx-female mice for any strain. SuHx-WT male mice demonstrated increased endothelial cell proliferation compared to WT-Control mice. These data suggest that the IL-33-receptor, ST2, and MyD88 signaling may play a role in the PAH vascular remodeling and disease progression. Further understanding of IL-33-mediated signaling that regulates endothelial cell proliferation, remodeling and cytokine activation may provide a better understanding of the disease and its advancement and allow the design of new treatment strategies for PAH.

INTRODUCTION

Pulmonary arterial hypertension

Pulmonary arterial hypertension (PAH) is a rare multifactorial cardiopulmonary disorder with about 15-50 cases per million (Peacock et al., 2007; Schermuly et al., 2011; Semen et al., 2016). This severe form of pulmonary hypertension is progressive and eventually leads to right heart failure and premature death (Demerouti et al., 2013). PAH is characterized by occlusive arteriopathy that is associated with high resting right ventricular pressures (RVP), greater than or equal to 25 mmHg, and increased pulmonary vascular resistance (PVR), greater than three Woods Units (240 dyn.s.cm-5), much higher than the average range of 0.3 – 1.6 Woods Units (Voelkel et al., 2012; Simonneau et al., 2013). This rise in RVP and PVR results from extensive cellular proliferation that leads to obliterative alterations in both structure and function of the endothelium, which are primarily prevalent in the small to midsized pulmonary arterioles (Schermuly et al., 2011; Rabinovitch et al., 2014).

Current treatments and therapies for PAH

Treatment of PAH is complex and will optimally involve a range of options aiming to relieve symptoms, delay disease progression and improve the resulting physical limitations (Barst et al., 2009). For example, supplemental oxygen has been used as a therapy to improve comfort and provide symptomatic relief. Oral anticoagulants may also be prescribed to patients with idiopathic PAH (IPAH), as they are prone to *in situ* thrombosis due to the narrowing of the small pulmonary arteries. Diuretics may also be used to alleviate symptoms in fluid-overloaded patients with decompensated right heart failure associated with PAH. For patients with advanced and severe forms of PAH, surgery may be the only remaining option. In these cases, a balloon atrial septostomy may be performed in which a small hole is created between the right and left atria to allow blood to pass directly over to the left heart. While this effectively improves

systemic oxygen transport, and thus decreases the pressure on the heart, it also results in hypoxemia. When all else fails, lung or lung and heart transplantation may be the only options that remain (Galiè et al., 2004; Galiè et al., 2009; Badesch et al., 2007).

In recent years, the focus has been greatly shifted towards the perivascular inflammation and cell proliferation that is often observed in patients with PAH. These therapies focus on dilating the partially occluded vessels, and they may target pathways that increase production of nitric oxide (Pepke-Zaba et al., 1991). Other treatments may target endothelin, a vasoconstrictor that promotes cell growth within blood vessels and results in lesions, by using drugs called endothelin receptor antagonist which function as weak antiproliferative agents by blocking its receptors. However, even with the currently available therapies, mortality remains high, and no therapy has been able to inhibit or reverse the pulmonary vascular remodeling and occlusive arteriopathy characteristic of PAH. To date, there is no cure for PAH and prognosis remains poor, but inflammatory mechanisms have been implicated in playing a role (Rabinovitch et al., 2014; Jafri et al., 2017).

Immunity, inflammation and interleukin-33: in the role of PAH

A wealth of research has indicated that immunity and inflammation play a crucial role in the pathogenesis of PAH (Jafri et al., 2017). In fact, studies in experimental PAH models have suggested that inflammation precedes vascular remodeling and is thus a cause rather than a consequence of PAH (Tamosiuniene et al., 2011). Beyond these findings, studies have also observed that certain cytokines, including interleukin (IL)-1β, IL-6, and IL-8, are abnormally elevated in PAH patients, may be indicative of disease progression, and thus may function as important biomarkers not only for PAH but other cardiovascular diseases as well (Soon et al.,

2010). Furthermore, members of our group previously measured elevated levels of IL-33 in the serum of patients with Group 1 PAH.

IL-33 is a cytokine and member of the IL-1 superfamily whose members have essential functions in host defense, immune regulation and inflammation. A key player in innate and adaptive immunity, IL-33 can initiate a plethora of biological effects all directed towards the restoration of tissue homeostasis and in response to environmental stresses (Liew et al., 2016; Braun et al., 2018). More specifically, IL-33 has been shown to act as an alarmin, a "danger" signal, and is constitutively expressed by endothelial and epithelial cells of barrier tissues, such as the lung, which release IL-33 in response to damage, injury or necrosis (Moussion et al., 2008; Cayrol et al., 2018). Since its discovery, it became evident that IL-33 plays a vital role in tissue homeostasis; however, uncontrolled and inappropriate activity can have deleterious effects. Recent studies have demonstrated a link between IL-33 administration or overexpression to fibrotic diseases (Li et al., 2014). For example, activation of IL-33 signaling can either repair the endothelial layer or, if the danger signals persist, contribute to uncontrolled proliferation and the initiation of an amplified cytokine response (Demyanets et al., 2011).

IL-33 signaling

IL-33 is produced as a 30–kDa precursor that when cleaved by caspase-1 is released as an 18–kDa mature form (Choi et al., 2009). Its signaling begins when it is bound by the receptor suppressor of tumorigenicity 2 (ST2), which plays an important role as an effector molecule of T helper type 2 responses (Schmitz et al. 2005). Binding of IL-33 to ST2L results in ST2 signaling that is characteristic of the Toll-like receptor-IL-1 receptor (TLR-IL-1R) superfamily (O'Neill et al., 2007; Lott et al., 2015).

When IL-33 binds to ST2, it induces a conformational change that allows the receptor to recruit IL-1 receptor accessory protein (IL-1RAcP), a co-receptor shared with other IL-1 family members, including IL-1 and IL-36, leading to the formation of a heterodimeric signaling complex (Liu et al., 2013). This complex is then able to induce signaling through recruitment of myeloid differentiation primary response protein 88 (MyD88), IL-1R-associated kinase 1 (IRAK1), IRAK4, and tumor necrosis factor (TNF) receptor-associated factor (TRAF6), that ultimately activate mitogen-activated protein kinases (MAPKs), such as extracellular signal-regulated kinase (ERK), p38, c-Jun N-terminal kinase (JNK), and nuclear factor-κB (NF-κB), a transcription factor for many proinflammatory genes (Schmitz et al., 2005). This signaling cascade results in proliferation, cell survival, type 2 cytokine secretion, IL-5 and IL-13, and amphiregulin (AREG) expression by ST2+ cells all of which support wound healing, tissue repair, as well as enhance immune regulatory functions by activation of a potent inflammatory response (Poynter et al., 2002; Schmitz et al., 2005; Price et al., 2010; Lott et al., 2015; Liew et al., 2016; Schwartz et al., 2016).

Inhibition of IL-33 signaling may be carried out by binding of soluble ST2 (sST2) to IL-33 that then prevents its signaling (Boraschi et al., 2018). Another way is through phosphorylation and ubiquitylation of ST2 that leads to its internalization and degradation (Liew et al., 2016). Moreover, studies have shown that ST2 gene deficiency results in a delayed immune response to lung damage and generation of T helper type 2 (T_H2) cytokine responses (Townsend et al., 2000). It should be noted that IL-33 is not the only ligand for this receptor and that two other putative ligands have been reported; however, neither of these two can activate NF-κB, nor are they members of the IL-1 cytokine family (Gayle et al., 1996).

As we have just described, MyD88 is an essential player in IL-33's signaling pathway. Previously, members of our group studied a MyD88 gene-deficient mouse strain (MyD88 -/-) to gain insight into the effect of this common adaptor protein in the signaling of many Toll-like receptors (TLR). It was known that all TLRs contain TLR/IL-1 receptor resistance (TIR) domains. Their studies were able to define a surface on these TIR domains that is responsible for not only mediating the association between TLRs and MyD88, but that is also required for their oligomerization. These findings suggested that MyD88 interacts with individual TLRs in a specific manner, making it a compelling target for TIR domain receptor blockade that could potentially render them powerless (Jiang et al., 2006).

We have described the signaling pathway for IL-33 and how it ultimately results in activation of an inflammatory response. We have also touched on the fact that it is expressed and secreted by endothelial cells, but in fact, studies have reported that IL-33 is highly expressed by endothelial cells and thus have an important relationship (Carriere et al., 2007; Küchler et al., 2008; Moussion et al., 2008; Liew et al., 2010). As such, our focus will now shift towards endothelial cell expression of IL-33 and how it relates to PAH.

A closer look at endothelial cells and PAH

Severe PAH is characterized by structural changes to the small pulmonary arterioles. These changes that result in the remodeling of the pulmonary vasculature are thought to be the result of endothelial cell proliferation (Tuder et al., 1994; Sakao et al., 2009). In endothelial cells, IL-33 has been shown to activate an inflammatory response which is evident through the increase in inflammatory cytokine production, vascular permeability, expression of adhesion molecules, stimulation of angiogenesis, and a decrease in cell stability (Choi et al., 2009; Demyanets et al., 2011; Chalubinski et al., 2015); Umebashi et al., 2018). Other studies have also

reported that IL-33 secretion by endothelial cells was crucial in converting myocardial pressure overload into a selective systemic inflammatory response and that it could potentially affect the vasculature and other organs (Chen et al., 2015). A study on pulmonary artery endothelial cells (PAEC) derived from IPAH compared these to those from healthy human lungs. This group observed that PAEC from IPAH where higher in number, had decreased apoptosis increased migratory behavior when compared to those from healthy lungs (Masri et al., 2007). Interestingly, a recent study by Suresh *et al.* focusing on the mechanisms that lead to endothelial cell dysfunction in PAH reported that lung microvascular endothelial cells (MVEC) from a SuHx rat PAH model were not only larger but also expressed smooth muscle cell markers. Here, in addition to the enhanced proliferative and migratory phenotypes, they also reported that SuHx-MVEC had dysfunctional mitochondria. This group showed that treatment with global or mitochondria-specific antioxidants led to a decrease in both migration and proliferation of SuHx-MVEC as ROS levels and basal calcium levels were decreased (Suresh et al., 2018).

Thus, in this study, we hypothesized that pulmonary vascular remodeling in PAH is regulated by an IL-33-dependent pathway that initiates hyperproliferation of the vascular endothelial cells and that inefficient downregulation of IL-33 activity could contribute to the aberrant vascular remodeling characteristic of PAH. To test this hypothesis, we used the current best murine model for pulmonary arterial hypertension, the Sugen 5416/Hypoxia model.

Much remains to be understood about the role of IL-33 in the progression of PAH. In this study, we report that IL-33 may have an important effect on PAH through an ST2/MyD88 pathway. This effect was studied by monitoring right ventricle pressures and cardiac function through right heart catheterization in groups exposed to Sugen 5416/Hypoxia treatment and compared these to the control, DMSO/RA, groups. We also measured pulmonary vascular

remodeling across all groups using histological techniques. Lastly, we assessed pulmonary endothelial cell proliferation after exposure to treatment and control conditions.

MATERIALS AND METHODS

Animals. All animal protocols were reviewed, approved and monitored by the Institutional Animal Care and Use Committee of the Veterans Administration San Diego Healthcare System (VASDHS) (VA Medical Center, La Jolla). Mouse strains included male and female C57BL/6J (wild-type: WT) mice purchased at 8-10 weeks of age from the Jackson Laboratory (Bar Harbor, ME).

An ST2 deficient mouse strain (ST2 -/-) was used to investigate the role that IL-33 plays in the progression of PAH. This ST2 -/- strain lacks the soluble, sST2, and membrane-bound, ST2L, forms of the ST2 receptor that bind to IL-33. These mice were obtained from Dr. Kenji Nakanishi (Hyogo College of Medicine, Hyogo, Japan) (Hoshino et al., 1999). Since the effect of ST2 in a PAH model was unknown, our goal was to further understand the role this receptor plays in IL-33 signaling in the development of PAH.

A MyD88 deficient mouse strain (MyD88 -/-) originally developed and provided by Dr. Shizuo Akira (Osaka University, Osaka, Japan) (Adachi et al., 1998) was used to study the role of this adaptor protein in the progression of PAH.

WT and mutant strains were housed and bred within the Barrier Facility at the VASDHS (VA Medical Center, La Jolla), maintained under standard laboratory conditions with controlled temperatures, fed a standard diet, Teklad 7001, *ad libitum*, from Harlan Laboratories (Madison, WI), and kept under a 12-hour dark and light cycle. Mice used in this study were harvested at 3.25 - 4 months of age. All mouse lines are on a C57BL/6J background strain.

Development of the Tek-Cre:: *IL33*$^{fl/fl}$ mouse. The constitutive, endothelial cell-specific *IL33* deficient mouse model was generated using the following transgenic mouse lines: A homozygous *IL33* floxed mouse, provided by Dr. Richard Lee (Harvard Medical School, Boston,

MA) (Chen et al., 2015), was intercrossed with a heterozygous Tie2-Cre(+/-) transgenic mouse that expresses Cre recombinase under the regulation of an endothelial-specific, Tie2 (also referred to as Tek), promoter/enhancer (Kisanuki et al, 2001).

In the *IL33* floxed mouse, the Cre-*lox*P system was employed to develop *IL33* conditional mutant mice by introducing two *lox*P sites into the *IL33* locus that flanks exons five through seven. Tek is a tyrosine receptor kinase that is the angiopoietin receptor that is expressed in endothelial cells. Thus, the promoter of this gene will restrict expression of the fused Cre recombinase protein to express only in endothelial cells such that when we cross an *IL33* floxed mouse with a heterozygous Tek-Cre (+/-) mouse, *IL33* will be selectively deleted in endothelial cells. The resulting mouse is what we refer to as a Tek-Cre(+/-)::$IL33^{fl/fl}$ mouse. The Tek-Cre(-/-)::$IL33^{fl/fl}$ littermates that lack the Cre recombinase gene were used as controls in this study. Tek-Cre(+/-) mice were purchased from the Jackson Laboratory (*stock no. 008863*, Bar Harbor, ME) and backcrossed five times on a C57Bl/6J background. Of the 68 mice used for the Tek-Cre::$IL33^{fl/fl}$ mouse line, 33 were positive (Tek-Cre(+/-)), and 35 were negative (Tek-Cre(-/-)). All were homozygous *IL33* floxed mice.

Genotyping was performed by PCR amplification of tail DNA isolated using hot sodium hydroxide and Tris HotShot lysis (Truett et al., 2000). The PCR primers for the floxed *IL33* alleles were forward 5'-aacctcctggtcaatattcagt-3' and reverse 5'- ccgcctactgcgactataga-3'. The PCR primers for the wild-type *IL33* alleles were forward 5'- caagtctggtctccagcaac-3' and reverse 5'-agcaagaacggaccagatgta-3'. The PCR primers for Cre recombinase were forward 5'-gcggtctggcagtaaaaactatc-3' and reverse 5'- gtgaaacagcattgctgtcactt-3'. The PCR primers for internal controls were forward 5'- ctaggccacagaattgaaagatct-3' and reverse 5'-gtaggtggaaattctagcatcatcc-3'. PCR amplification of the floxed and wild-type IL-33 transgenes

was performed with the following program: 60 seconds at 94°C for polymerase activation, 35 cycles of 30 seconds at 94°C for denaturation, 30 seconds at 59°C for annealing, 60 seconds at 72°C for elongation, and five minutes at 72°C for a single final extension. The PCR conditions for the Cre recombinase transgene differed from those described previously as follows: a three-minute incubation at 94°C for polymerase activation, 60 seconds at 51.7°C for annealing, and two minutes at 72°C for a single final extension. All PCR products were loaded onto 1.5% agarose (Sigma-Aldrich) gels containing SYBR ® Safe DNA gel stain (Invitrogen, by Thermo Fisher Scientific) and electrophoresed in 1X Tris-Acetate-EDTA (TAE) buffer for analysis and confirmation of genotypes.

Hypoxia/Sugen 5416 mouse model. To investigate the role of IL-33 in PAH, we used the current best mouse model that leads to an exaggerated form of pulmonary hypertension (PH), the Sugen 5416 (SU5416) and hypoxia model (Ciuclan et al., 2011). WT and mutant mice were exposed to chronic hypoxia (10% O_2) for three weeks in a hypoxia chamber (Biospherix, Lacona, NY) and received weekly subcutaneous (S.C.) injections of SU5416 (20 mg/ kg in DMSO; Cayman Chemical) to induce PAH, or they were exposed to room air conditions (21% O_2) and given weekly S.C. injections of vehicle, DMSO, as the control condition. SU5416, also referred to as Semaxanib, is a potent synthetic inhibitor of the vascular endothelial growth factor (VEGF) receptor tyrosine kinase that targets the VEGF pathway. *In vivo* and *in vitro* studies have demonstrated SU5416's antiangiogenic potential, indicating that it inhibits normal endothelial cell growth and homeostasis (Fong et al., 1999). SU5416 (50 mg) was dissolved in 5 ml of DMSO, aliquoted and stored at -80° C. Each mouse was weighed prior to harvest.

***In vivo* measurements of right ventricular pressures.** Mice were anesthetized by continuously delivering 2.5% isoflurane through a nose cone, and their body temperature was maintained at 37°C. The right jugular vein was exposed, and 3-0 silk sutures were used to tie off the distal part of the vein and to loosely wrap around the proximal region. At this point, mechanical ventilation of the mouse was reduced to deliver 1.5% isoflurane. A small incision was made between the two sutures, and the vein was cannulated using a 1.4-French microtip pressure transducer (Millar SPR839, Millar Instruments, Houston, TX). The transducer was then advanced into the right ventricle until wave tracings were identified. The transducer was then secured with the distal suture and pressures were continuously monitored and recorded. Data were analyzed with an Emka IOX version 1.8 software program (Emka Technologies, Falls Church, VA). Upon completion of data collection, mechanical ventilation was increased to place mice under deep anesthesia, a median sternotomy was performed to access the heart, and mice were exsanguinated by cardiac puncture for blood collection which was then processed for future analysis.

Perfusion and embedding of lung tissue. Immediately after harvest, the left atrium was excised, the pulmonary artery was cannulated, and lungs were perfused with PBS for two minutes. The left lung was then isolated, removed and flash frozen for future analyses. The right lung was inflated and fixed with 0.75 ml of 10% formalin instilled through the trachea and stored in 10% formalin overnight. Lungs were then dehydrated and embedded in paraffin.

Pulmonary arterial (PA) wall thickness. To quantitate PA wall thickness, the paraffin-embedded right lobes of the lung were cut into 5 μm thick sections, stained with hematoxylin

and eosin (H&E), and slides were scanned with a Hamamatsu 2.0-HT Nanozoomer Slide Scanning System (Hamamatsu Corporation, Bridgewater, NJ) at the UCSD Microscopy Core (La Jolla, CA). The total vascular area at the adventitial border and the lumen area at the basement membrane were outlined and measured using the Nanozoomer Digital Pathology NDP.view2software. The PA wall thickness in arteries with 50-100 μm diameter was calculated as follows: wall thickness = (total vascular area – lumen area)/total vascular area. Data are presented as changes as a ratio of wall area to total vessel area (Ma et al., 2011).

Detection of actively proliferating endothelial cells in lung tissue. To assess and confirm pulmonary endothelial cell proliferation in our SU5416/Hypoxia murine model, mice were injected intraperitoneally (I.P.) with 5-bromo-2′deoxyuridine (BrdU, B5002 Sigma) at a dose of 50 mg/kg body mass for seven consecutive days prior to harvest. The left pulmonary lobe was removed, minced, and digested with Collagenase and DNase type 1 from Sigma-Aldrich added to a final concentration of 0.2% and 100 μg/ml, respectively, in DMEM (GIBCO). Samples were incubated while gently shaking at 37°C for 30-45 minutes. A cell suspension was made by passing the digested lungs through a 40 μm cell strainer (BD Falcon) and washing by centrifugation. The cells were stained for flow cytometry (Guava easyCyte 8HT; Millipore, Boston, MA) using standard procedures for antibodies. Antibodies used: anti-CD31 (dilution 1:100, Cat. No. 550274, BD Pharmingen, Franklin Lakes, NJ), CD31 FITC (dilution 1:100, clone 390, 11-0311-82, eBioscience) and anti-BrdU (dilution 1:100, clone: BU20A, eBioscience)-PE. Flow cytometry data were analyzed using the FlowJo Software (Tri Star Inc., Ashland, OR).

Statistical analyses. A two-way ANOVA was used to detect differences between the genotypes and conditions, followed by Tukey's *post-hoc* tests to identify specific differences in body weight, hemodynamic parameters and PA wall thickness between the experimental groups. Student's t-test was used to compare the average percentage of BrdU+ and CD31+ cells in control, DMSO/RA, and SuHx groups when only WT male mice were used. Data are represented as means ± SD. A value of $P < 0.05$ was considered a significant difference. Data were analyzed using Prism (Graph Pad, San Diego, CA) software.

RESULTS: CHAPTER I

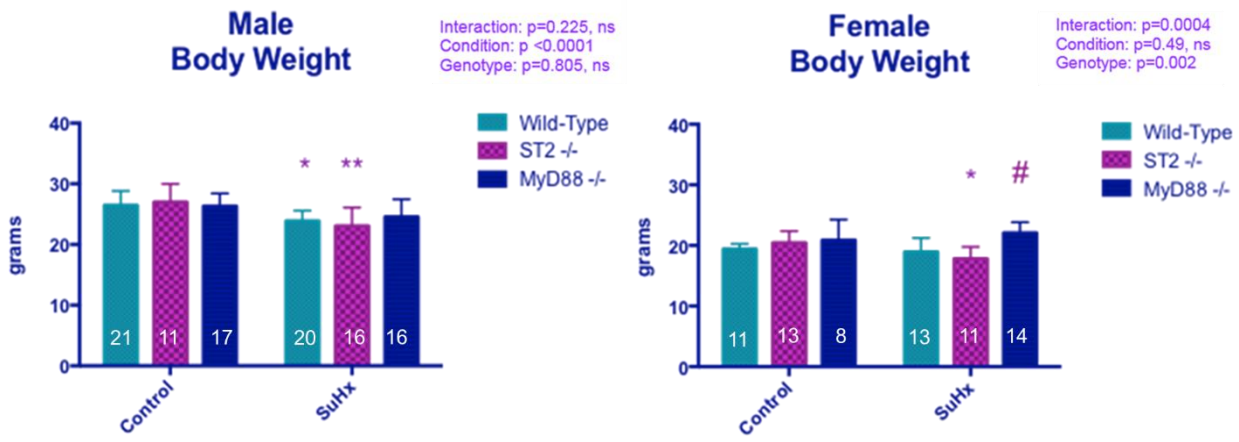

Figure 1: Body weight was preserved in male and female MyD88 -/- mice exposed to SU5416/Hypoxia (SuHx). * indicates a difference between treatment groups for the same genotype. # indicates a difference between genotypes under the same conditions. Male mice, n = 9-23. Female mice, n = 6-15. $P < 0.05$.

Body weight. We compared body weight changes in ST2 -/- and MyD88 -/- mice to that of C57BL/6J, wild-type (WT) mice. Figure 1 shows that body weight was decreased by 11% in WT and 15% in ST2 -/- males, but not in MyD88 -/- male mice after the three-week chronic exposure to 10% oxygen and weekly s. c. injections of SU5416 (SuHx), (Control vs SuHx males; WT: 26.44 ± 2.37 g vs. 23.89 ± 1.71 g, $P < 0.05$; ST2 -/-: 27.00 ± 2.99 g vs. 23.05 ± 3.02g, $P \leq 0.01$; MyD88 -/-: 26.33 ± 2.09 g vs. 24.54 ± 2.93 g, P = NS). Only ST2 -/- females lost 12% of their body weight under SuHx conditions (Control vs SuHx females; WT: 19.41 ± 0.88 g vs. 18.95 ± 2.28 g, P = NS; ST2 -/-: 20.44 ± 1.93 g vs. 17.82 ± 1.98 g, $P \leq 0.05$; MyD88 -/-: 20.87 ± 3.43 g vs. 22.07 ± 1.79 g, P = NS). Under SuHx conditions, female MyD88 -/- mice were able to significantly preserve their body weight compared to WT females ($P \leq 0.01$) and ST2 -/- females ($P \leq 0.0001$).

A

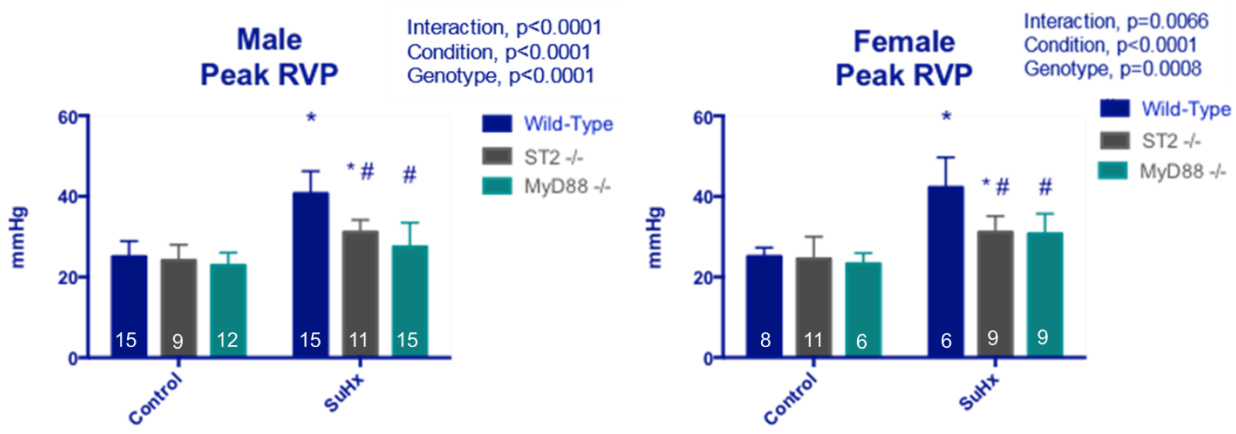

B

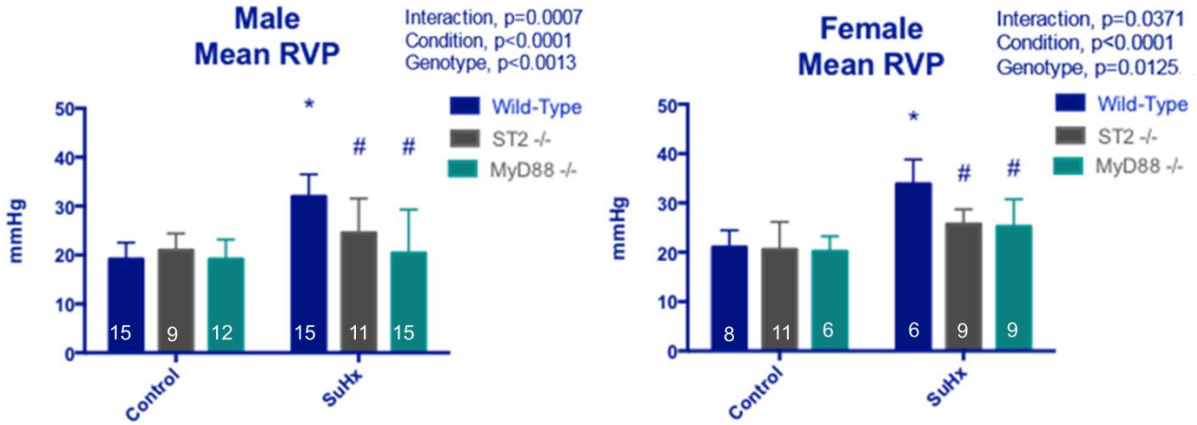

Figure 2: Right ventricle pressures are attenuated in mice that do not express the IL-33 receptor, ST2, or the upstream innate immune adaptor protein, MyD88. (A) Peak RVP. (B) Mean RVP. * indicates a difference under SuHx conditions within the same genotype. # indicates a difference compared to the other genotypes under the same condition. Male mice, n = 9-15. Female mice, n = 6-11. $P < 0.05$.

Right ventricular pressures were attenuated in ST2 -/- and MyD88 -/- mice. We assessed the effect of SuHx on anesthetized mice through right heart catheterization by measuring and monitoring their peak and mean right ventricular pressures using a pressure-conductance transducer. Figure 2A shows that compared with mice maintained in control

conditions, WT mice exposed to SuHx peak RVP increased by 63%. In ST2 -/- mice peak RVP increased yet these values were still 30% lower than that of WT-SuHx mice. In MyD88 -/- mice, peak RVP did not increase. Male peak RVP (Control vs. SuHx males; WT: 25.03 ± 3.88 mmHg vs. 40.68 ± 5.54 mmHg, $P < 0.0001$; ST2 -/-: 24.09 ± 3.90 mmHg, vs 31.08 ± 3.07 mmHg, $P < 0.05$; MyD88 -/-: 22.86 ± 3.20 mmHg vs. 27.43 ± 6.03 mmHg, P = NS). Female peak RVP increased by 68%, whereas in ST2 -/- females there was only a 19% increase, and in MyD88 -/- females, no increase was observed (Control vs. SuHx females; WT: 25.07 ± 2.22 mmHg vs. 42.24 ± 7.44 mmHg, $P < 0.0001$; ST2 -/- 24.50 ± 5.48 mmHg vs 31.08 ± 4.04 mmHg, $P < 0.05$; MyD88 -/-: 23.22 ± 2.69 mmHg vs. 30.66 ± 5.00 mmHg, P = NS). Figure 2B shows that when we evaluate mean RVP, we detect a 68% increase in WT-SuHx mice compared to control conditions. ST2 -/- mice revealed attenuated responses to SuHx that were evident in mean RVP, as we did not observe a significant difference compared to the control condition. MyD88 -/- mice did not show an increase in mean RVP either. Male mean RVP (Control vs. SuHx males; WT: 19.15 ± 3.37 mmHg vs. 31.99 ± 4.48 mmHg, $P < 0.0001$; ST2 -/-: 20.96 ± 3.46 mmHg vs. 24.53 ± 7.01 mmHg, P = NS; MyD88-/-: 19.14 ± 4.02 mmHg vs. 20.42 ± 8.88 mmHg, P = NS). Female mean RVP (Control vs. SuHx females; WT: 21.04 ± 3.43 mmHg vs. 33.87 ± 4.94 mmHg, $P < 0.0001$; ST2 -/-: 20.55 ± 5.60 mmHg vs. 25.70 ± 3.00 mmHg, P = NS; MyD88 -/-: 20.19 ± 3.06 mmHg, SuHx 25.21 ± 5.56 mmHg; P = NS). Under SuHx conditions, male ST2 -/- mice significantly attenuated peak ($P < 0.0001$) and mean ($P < 0.05$) RVP compared to WT-SuHx male mice. Similarly, female ST2 -/- mice demonstrated attenuated peak ($P < 0.001$) and mean ($P < 0.01$) RVP compared to WT-SuHx female mice. There was no significant difference between males and females for any genotype under control or SuHx conditions.

Table 1: Hemodynamic variables of C57Bl/6J (WT), ST2 -/-, and MyD88 -/- male mice with and without SU5416/Hypoxia (SuHx) exposure.

Hemodynamic data	WT Control	WT SuHx	ST2 -/- Control	ST2 -/- SuHx	MyD88 -/- Control	MyD88 -/- SuHx
RVSP, mmHg	23.21 ± 3.39	38.42 ± 5.48 ****	23.58 ± 3.84	28.86 ± 6.84 #	22.31 ± 3.47	23.32 ± 10.25 #
RVDP, mmHg	27.04 ± 2.94	40.52 ± 6.25 ****	24.96 ± 4.26	29.61 ± 6.90 #	25.69 ± 2.93	30.69 ± 5.94 #
RV dP/dt_{max}, mmHg/sec	2119.73 ± 431.47	2863.85 ± 759.89 *	2065.07 ± 481.87	1868.43 ± 510.70 #	1862.77 ± 509.78	1997.19 ± 772. 28 #
RV dP/dt_{min}, mmHg/sec	-1800.43 ± 425.67	-2494.48 ± 578.37 **	-1710.32 ± 287.47	-1618.31 ± 566.41 #	-1532.18 ± 508.98	-1519.43 ± 675.83 #
HR, beats per min	506.37 ± 66.14	470.13 ± 84.07	504.70 ± 32.74	421.34 ± 52.83	436.67 ± 91.39	435.47 ± 119.53

Right ventricular (RV) pressures are expressed as follows: RV end-systolic pressure (RVSP); RV developed pressure (RVDP); RV dP/dt_{max} (instantaneous rate of contraction) and RV dP/dt_{min} (instantaneous rate of relaxation). Note: Data are represented as mean values ± standard deviations. * indicates a difference under SuHx conditions within the same genotype. # indicates a difference compared to the other genotypes under the same condition. Male mice, n = 9-15. * indicates $P< 0.05$, ** indicates $P < 0.01$, *** indicates $P < 0.001$ and **** indicates $P <0.0001$.

Protection of cardiac function in ST2 -/- and MyD88 -/- mice. To further assess the effect of chronic SuHx exposure of male mice on cardiac function we also monitored and measured other hemodynamic parameters through right heart catheterization using a pressure-conductance catheter. Table 1 shows that heart rates were not different in any mouse group under any condition. A significant increase of 65% in right ventricular (RV) end-systolic pressure (RVSP), 50% in RV developed pressure (RVDP), 35% in RV contractility (RV dP/dt_{max}) and 39% RV relaxation (RV dP/dt_{min}) was observed in W-SuHx mice compared to ST2 -/- and MyD88 -/- mice in which no difference was observed after SuHx exposure. Chronic SuHx

exposure had an effect on right heart cardiac function in WT male mice, but there were no significant changes in either ST2 -/- or MyD88 -/- mice.

Table 2: Hemodynamic variables of C57Bl/6J (WT), ST2 -/-, and MyD88 -/- female mice with and without SU5416/Hypoxia (SuHx) exposure.

Hemodynamic data	WT Control	WT SuHx	ST2 -/- Control	ST2 -/- SuHx	MyD88 -/- Control	MyD88 -/- SuHx
RVSP, mmHg	24.28 ± 3.29	41.53 ± 6.87 ****	23.40 ± 5.85	29.98 ± 4.69 #	22.89 ± 2.93	27.07 ± 8.54 #
RVDP, mmHg	25.75 ± 3.33	43.78 ± 7.36 ****	25.27 ± 3.46	32.80 ± 4.87 * #	24.88 ± 2.46	30.31 ± 7.07 #
RV dP/dt_{max}, mmHg/sec	1733.48 ± 420.64	2986.39 393.26 ***	1876.37 ± 635.06	2689.48 ± 411.64 ** #	1714.43 ± 273.38	2276.03 ± 465.35 #
RV dP/dt_{min}, mmHg/sec	-1432.37 ± 502.79	-2674.21 ± 441.79 ****	-1502.84 ± 437.80	-2337.12 ± 605.92 * #	-1463.94 ± 247.44	-2015.81 ± 692.70 #
HR, beats per minute	428.22 ± 80.16	417.37 ± 46.98	460.72 ± 46.31	481.99 ± 26.91	413.80 ± 52.98	466.91 ±52.67

Right ventricular (RV) pressures are expressed as follows: RV end-systolic pressure (RVSP); RV developed pressure (RVDP); RV dP/dt_{max} (instantaneous rate of contraction); and RV dP/dt_{min} (instantaneous rate of relaxation). Note: Data are represented as mean values ± standard deviations. Female mice, n = 6-11. * indicates a difference between treatment groups for the same genotype. # indicates a difference between genotypes under the same conditions.

As shown in Table 2, among the female mouse groups, we also see no significant difference in heart rate for any group under any condition. As was seen in the male groups, after SuHx, RVSP significantly increased by 71% in WT female mice ($P < 0.0001$), yet no significant differences were measured for either ST2 -/- or MyD88 -/- females after SuHx compared to the control condition. In contrast, RVDP increased by 70% ($P < 0.0001$) in WT and 30 % ($P < 0.05$) ST2 -/- females after SuHx; however, in ST2 -/- females, RVDP was still significantly lower than that of WT females. In MyD88 -/- females, there was no significant difference in RVDP

compared to control mice. In WT-SuHx females, RV contractility (RV dP/dt_{max}) increased by 72%, whereas in ST2 -/- SuHx-females we saw an increase of 43% ($P < 0.01$). There was no significant difference in RV dP/dt_{max} in MyD88 -/- females after SuHx. Lastly, we measured the highest increase, 87%, in RV dP/dt_{min} for WT-SuHx females. In ST2 -/- females there was an increase of 55%, however, these were still significantly lower than WT females after SuHx. MyD88 -/- females did not have a significant increase in RV dP/dt_{min}.

Pulmonary vascular remodeling is attenuated in ST2 -/- and MyD88 -/- mice. To evaluate pulmonary vascular remodeling, the medial thickness of the small resistance arteries was measured after three weeks of chronic SuHx exposure. Figure 3A shows a 47% significant increase in the thickness of the pulmonary vascular walls of WT-SuHx male mice compared to WT mice with DMSO/RA. ST2 and MyD88 gene deletion attenuated this response. Data presented as changes in ratio of wall area to total vessel area in lung sections. Wall thickness (Control vs SuHx males; WT: 0.38 ± 0.05 vs. 0.56 ± 0.08, $P < 0.01$; ST2 -/-: 0.38 ± 0.05 vs. 0.46 ± 0.08, P = NS; MyD88 -/- 0.39 ± 0.05 vs. 0.41 ± 0.14, P = NS). In female mice, we do not see a significant increase in pulmonary vascular remodeling under SuHx compared to controls, nor do we see a significant increase in pulmonary vascular remodeling in ST2 -/- or MyD88 -/- female mice. However, wall thickness was significantly lower in MyD88 -/- females compared to WT and ST2 -/- mice after SuHx exposure. (Control vs SuHx females; WT: 0.34 ± 0.06 vs. 0.44 ± 0.06, P = NS; ST2 -/-: 0.37 ± 0.06 vs. 0.38 ± 0.03, P = NS; MyD88 -/-: 0.32 ± 0.01 vs. 0.34 ± 0.03, P = NS). Figure 3B shows representative images of lung sections of mice.

A

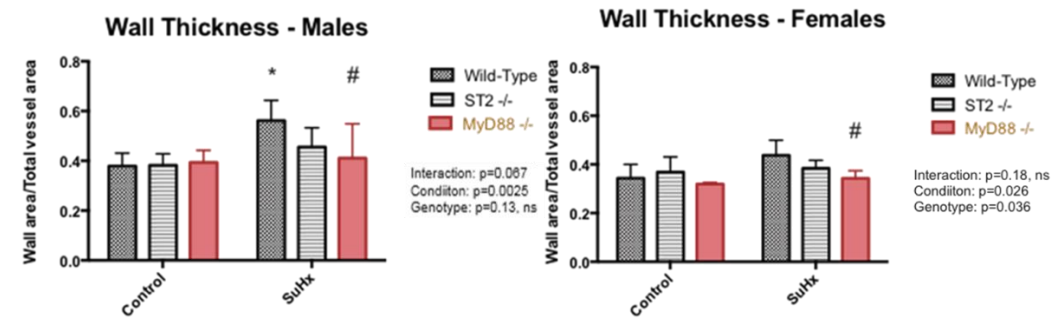

B

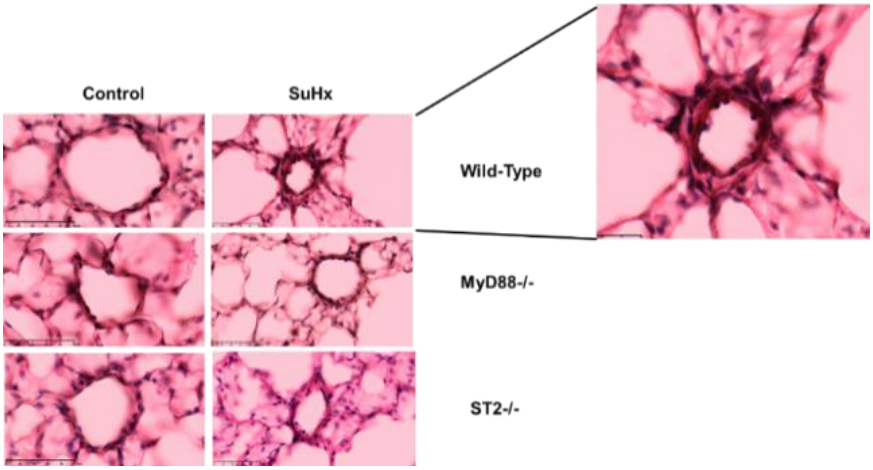

Figure 3: Mice that do not express the receptor, ST2, or the MyD88 adaptor protein show a decrease in the pulmonary vascular remodeling characteristic of pulmonary arterial hypertension. (A) Changes in ratio of wall area to total vessel area in the lung sections of mice. (B) Representative images of PAH mouse lung sections. Original magnification, ×400. *n* = 6. * indicates a difference between treatment groups for the same genotype. # indicates a difference between genotypes under the same conditions. $P < 0.05$.

Endothelial cell proliferation. There were no significant differences in control vs SuHx-WT male mice when we labeled for CD31+ or BrdU+ alone. However, we did measure a significant increase in actively proliferating cells within WT-SuHx mice when we analyzed cells that were both CD31+ and BrdU+ compared to controls (Control vs. SuHx; WT males: 3.21 ± 1.73 vs. 7.00 ± 4.47, P = 0.04).

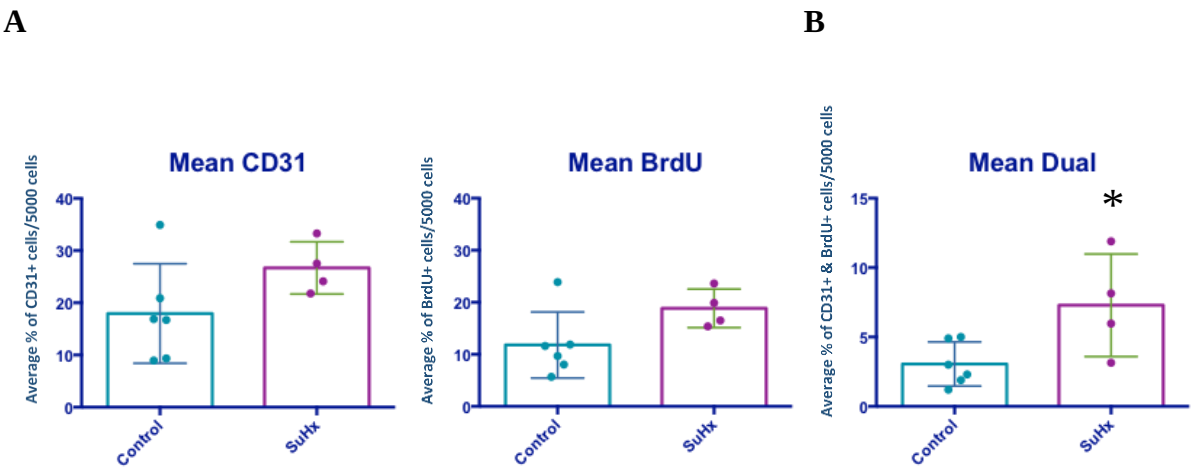

Figure 4: Isolation and enumeration of CD31+ and BrdU+ cells was determined by flow cytometry in male mice exposed to SuHx. Control, N = 6; SuHx, N = 4. Mean CD31+ and Mean BrdU+ (A) Mean dual labeling for CD31+ and BrdU+ cells (B). * Indicates a significant difference of $P < 0.05$. Data are represented as mean ± SD.

RESULTS: CHAPTER II

To gain insight into the role of *IL33* in endothelial cells, we generated a mouse line in which we inactivated *IL33* specifically in endothelial cells by crossbreeding two transgenic mouse lines.

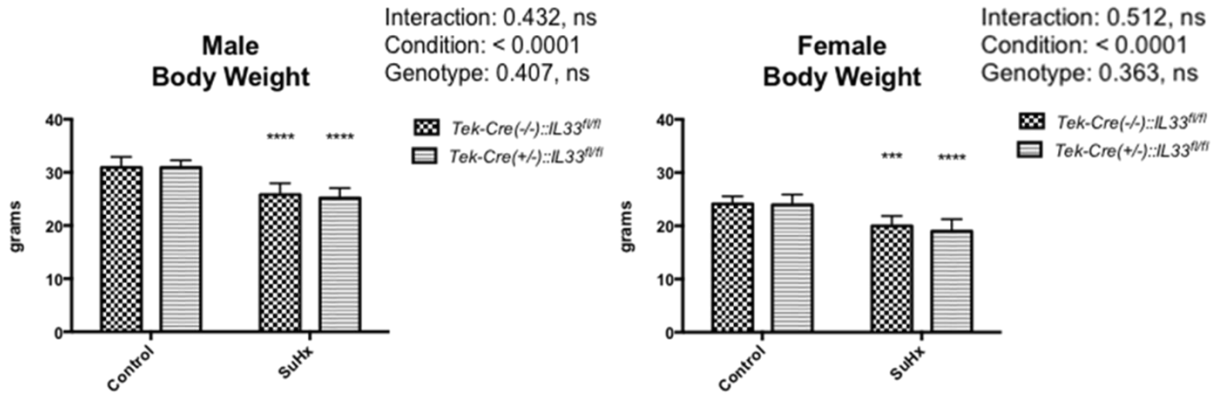

Figure 5: Both male and female Tek-Cre::*IL33*$^{fl/fl}$ mice weighed significantly less after exposure to SuHx conditions compared to DMSO/RA, control, groups. * indicates a difference between treatment groups for the same genotype. Male mice, n = 6-11. Female mice, n = 6-10. *** indicates P < 0.001 and **** indicates P < 0.0001.

Body weight. Figure 5 shows that both Tek-Cre(+/-)::*IL33*$^{fl/fl}$ male mice and their littermate controls weighed significantly less when exposed to three weeks of chronic SuHx conditions compared to DMSO/RA (control) groups; and, there was no significant difference in weight between Tek-Cre(+/-)::*IL33*$^{fl/fl}$ and Tek-Cre(-/-)::*IL33*$^{fl/fl}$ mice under SuHx. Body weight (Control vs. SuHx, males; Tek-Cre(-/-)::*IL33*$^{fl/fl}$: 30.92 ± 1.98 g vs. 25.82 ± 2.14 g, P < 0.0001; Tek-Cre(+/-)::*IL33*$^{fl/fl}$: 30.89 ± 1.35 g vs. 25.15 ± 1.87 g, P < 0.0001). Female Tek-Cre(+/-)::*IL33*$^{fl/fl}$ and their littermate controls also lost weight under SuHx compared to controls; however, no significant difference was observed between the genotypes after SuHx exposure. Body weight (Control vs. SuHx, females: Tek-Cre(-/-)::*IL33*$^{fl/fl}$: 24.10 ± 1.46 g vs. 19.99 ± 1.85 g, P < 0.0001; Tek-Cre(+/-)::*IL33*$^{fl/fl}$: 23.93 ± 1.93 g vs. 18.93 ± 2.28 g, P < 0.0001). These data

suggest that a conditional endothelial knockout of *IL33* does not result in a preventative measure against weight loss when under SuHx.

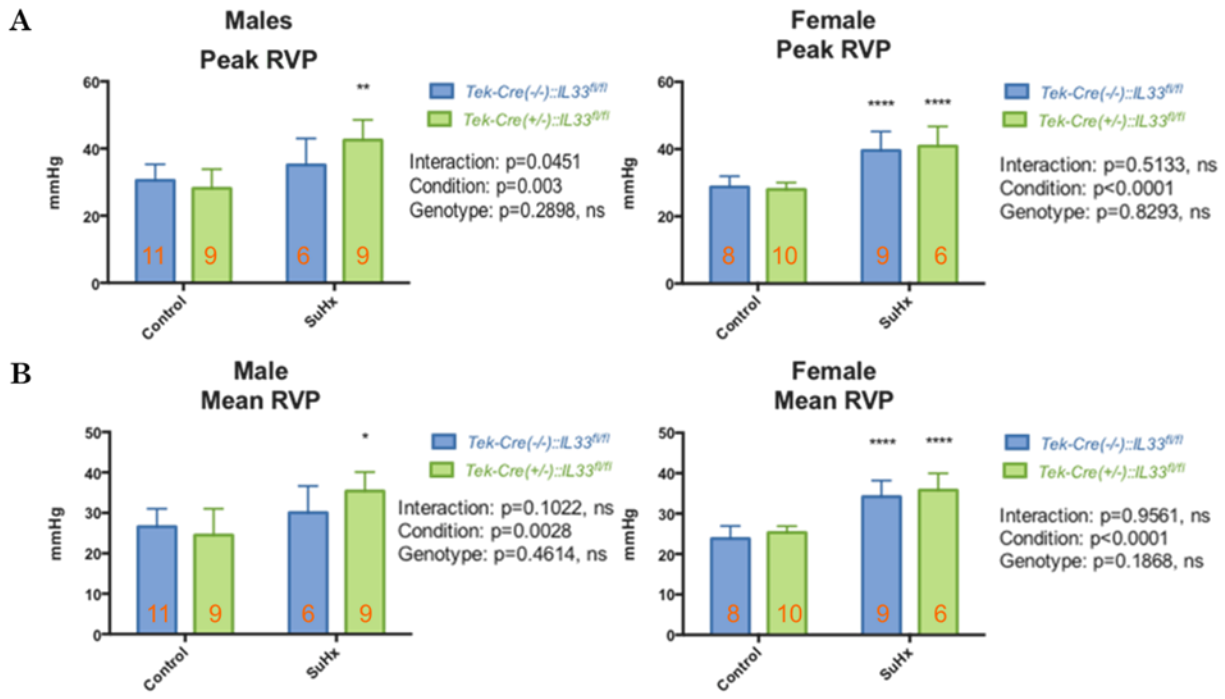

Figure 6: Mice with a conditional gene deletion of *IL33* in endothelial cells do not show a reduction in right ventricle pressures. Male and female (A) peak and (B) mean RVPs**.** * indicates a differenc · between treatment groups for the same genotype. Male, N = 6 – 11. Female, N = 6 – 10. * indicates P < 0.05, ** indicates P <0.01 and **** indicates P < 0.0001.

Right ventricular pressures were not attenuated in mice with a conditional *IL33* endothelial cell knockout. To further assess the effect of conditional endothelial cell *IL33* inactivation after SuHx exposure, peak and mean right ventricular pressures were monitored and measured through right heart catheterization. Figure 6 shows that there was a significant increase in peak and mean RVP in Tek-Cre(+/-)::*IL33*$^{fl/fl}$, male mice, but not in their littermate controls. Peak RVP (Control vs. SuHx, males; Tek-Cre(-/-)::*IL33*$^{fl/fl}$: 30.53 ± 4.80 mmHg vs. 35.11 ± 7.92

mmHg, P = NS; Tek-Cre(+/-)::*IL33*$^{fl/fl}$: 28.16 ± 5.72 mmHg vs. 42.52 ± 6.06 mmHg, P < 0.01) and Mean RVP (Control vs. SuHx, males: Tek-Cre(-/-)::*IL33*$^{fl/fl}$: 26.59 ± 4.43 mmHg vs. 30.05 ± 6.61 mmHg, P = NS; Tek-Cre(+/-)::*IL33*$^{fl/fl}$: 24.53 ± 6.48 mmHg vs. 35.39 ± 4.71 mmHg, P < 0.05). In females, there was an increase in peak and mean RVP for both littermate controls and Tek-Cre(+/-)::*IL33*$^{fl/fl}$ mice. Peak RVP (Control vs. SuHx, females; Tek-Cre(-/-)::*IL33*$^{fl/fl}$: 28.66 ± 3.20 mmHg vs. 39.55 ± 5.63 mmHg, P < 0.0001; Tek-Cre(+/-)::*IL33*$^{fl/fl}$: 27.99 ± 2.05 mmHg vs. 40.89 ± 5.84 mmHg, P < 0.0001) and Mean RVP (Control vs. SuHx, females; Tek-Cre(-/-)::*IL33*$^{fl/fl}$: 23.81 ± 3.12 mmHg vs. 34.20 ± 4.00 mmHg, P <0.0001; Tek-Cre(+/-)::*IL33*$^{fl/fl}$: 25.31 ± 1.57 mmHg vs. 25.81 ± 4.17 mmHg, P < 0.001). There was no difference between the two genotypes under any condition.

Effect of a conditional *IL33* endothelial cell knockout on cardiac function after SuHx exposure. To further assess the effect of a conditional endothelial *IL33* knockout on cardiac function, we monitored and measured other key hemodynamic parameters. Table 3 shows that there was no significant difference in heart rate for any group under any condition. Among the littermate controls, we saw no significant differences after three weeks of control or SuHx conditions for any parameter. In contrast, in male Tek-Cre(+/-)::*IL33*$^{fl/fl}$ mice, there were increases of 52% in RVSP (P <0.05), 55% in RVDP (P < 0.01), 59% in RV contractility (P < 0.05) and 72% increase in RV relaxation (P < 0.01) after SuHx exposure when compared to controls.

Table 3: Hemodynamic variables of Tek-Cre(-/-)::*IL33*$^{fl/fl}$ and Tek-Cre(+/-)::*IL33*$^{fl/fl}$ male mice with and without SU5416/Hypoxia (SuHx) exposure.

Hemodynamic data	Tek-Cre (-/-):: *IL33*$^{fl/fl}$ Control	Tek-Cre (-/-):: *IL33*$^{fl/fl}$ SuHx	Tek-Cre (+/-):: *IL33*$^{fl/fl}$ Control	Tek-Cre (+/-):: *IL33*$^{fl/fl}$ SuHx
RVSP, mmHg	30.08 ± 4.74	30.48 ± 12.66	27.44 ± 6.43	41.93 ± 4.95 *
RVDP, mmHg	26.31 ±5.00	33.22 ± 7.75	25.85 ± 5.11	40.16 ± 4.59 **
RV dP/dt_{max}, mmHg/sec	1978.55 ±507.42	2210.78 ± 696.15	1637.53 ± 472.57	2599.95 ± 561.85 *
RV dP/dt_{min}, mmHg/sec	-1615.56 ± 290.71	-1936.12 ± 633.35	-1395.14 ± 400.05	-2402.66 ± 633.08 **
HR, beats per min	406.26 ± 49.23	411.49 ± 30.17	393.15 ± 73.91	375.54 ± 12.56

Right ventricular (RV) pressures are expressed as follows: RV end-systolic pressure (RVSP); RV developed pressure (RVDP); RV dP/dt_{max} (instantaneous rate of contraction) and RV dP/dt_{min} (instantaneous rate of relaxation). Note: Data are represented as mean values ± standard deviations. * indicate a difference under SuHx conditions within the same genotype. Male mice, n = 6-11. * indicates $P < 0.05$, ** indicates $P < 0.01$, *** indicates $P < 0.001$ and **** indicates $P < 0.0001$.

In Table 4, we see that heart rates were not different after treatment, but we do see that all female Tek-Cre::*IL33*$^{fl/fl}$ mice responded more robustly to chronic SuHx exposure. In Tek-Cre(-/-)::*IL33*$^{fl/fl}$ females, there were increases of 59% in RVSP ($P < 0.0001$), 37% in RVDP ($P < 0.01$), 55% in RV contractility ($P < 0.05$) and 56 % in RV relaxation ($P < 0.01$) compared to controls after SuHx exposure. Similarly, Tek-Cre(+/-)::*IL33*$^{fl/fl}$ females demonstrated increases of 48% in RVSP ($P < 0.0001$), 48% in RVDP, 73% in RV contractility ($P < 0.01$), and 76% in RV relaxation ($P < 0.01$). There was so significant difference among the genotypes under the same treatment.

Table 4: Hemodynamic variables of Tek-Cre(-/-)::*IL33*$^{fl/fl}$ and Tek-Cre(+/-)::*IL33*$^{fl/fl}$ female mice with and without SU5416/Hypoxia (SuHx) exposure.

Hemodynamic data	Tek-Cre (-/-):: *IL33*$^{fl/fl}$ Control	Tek-Cre (-/-):: *IL33*$^{fl/fl}$ SuHx	Tek-Cre (+/-):: *IL33*$^{fl/fl}$ Control	Tek-Cre (+/-):: *IL33*$^{fl/fl}$ SuHx
RVSP, mmHg	24.53 ± 8.69	39.08 ± 5.16 ****	27.49 ± 2.22	40.74 ± 5.80 ****
RVDP, mmHg	26.66 ± 2.62	36.62 ± 6.47 **	26.21 ± 2.90	38.72 ± 6.47 ***
RV dP/dt_{max}, mmHg/sec	1564.01 ± 305.81	2429.88 ± 914.02 *	1466.51 ± 229.93	2541.63 ± 348.92 **
RV dP/dt_{min}, mmHg/sec	-1369.13 ± 295.87	-2135.14 726.46 **	-1251.01 ± 207.23	-2203.37 ± 341.57 **
HR, beats per min	400.57 ± 27.34	371.12 ± 70.56	371.81 ± 44.45	363.82 ± 29.87

Right ventricular (RV) pressures are expressed as follows: RV end-systolic pressure (RVSP); RV developed pressure (RVDP); RV dP/dt_{max} (instantaneous rate of contraction) and RV dP/dt_{min} (instantaneous rate of relaxation). Note: Data are represented as mean values ± standard deviations. * indicate a difference under SuHx conditions within the same genotype. Female mice, n = 6-10. ** indicates P<0.01 and **** indicates <0.0001.

Pulmonary vascular remodeling in Tek-Cre::*IL33*$^{fl/fl}$ mice. Figure 7 shows that after three weeks of chronic SuHx exposure, there was a significant increase in the thickness of the pulmonary vascular walls in both Tek-Cre(+/-)::*IL33*$^{fl/fl}$ male mice and their littermate controls compared to those in the control condition. The data are presented as changes in ratio of wall area to total vessel area in lung sections. Wall thickness (Control vs SuHx males; Tek-Cre(-/-)::*IL33*$^{fl/fl}$: 0.40 ± 0.04 vs. 0.60 ± 0.04, P < 0.0001; Tek-Cre(+/-)::*IL33*$^{fl/fl}$: 0.40 ± 0.02 vs. 0.54 ± 0.06, P < 0.01). There was no difference among the genotypes under any condition. Interestingly, in female Tek-Cre::*IL33*$^{fl/fl}$ mice, we do not see a significant increase in pulmonary vascular remodeling under SuHx compared to the control condition, nor do we see a significant difference among the genotypes under any condition. Wall thickness (Control vs SuHx females; Tek-Cre(-/-

)::*IL33*$^{fl/fl}$:: 0.44 ± 0.14 vs. 0.59 ± 0.04, P = NS; Tek-Cre(+/-)::*IL33*$^{fl/fl}$: 0.38 ± 0.03 vs. 0.49 ± 0.04, P = NS.

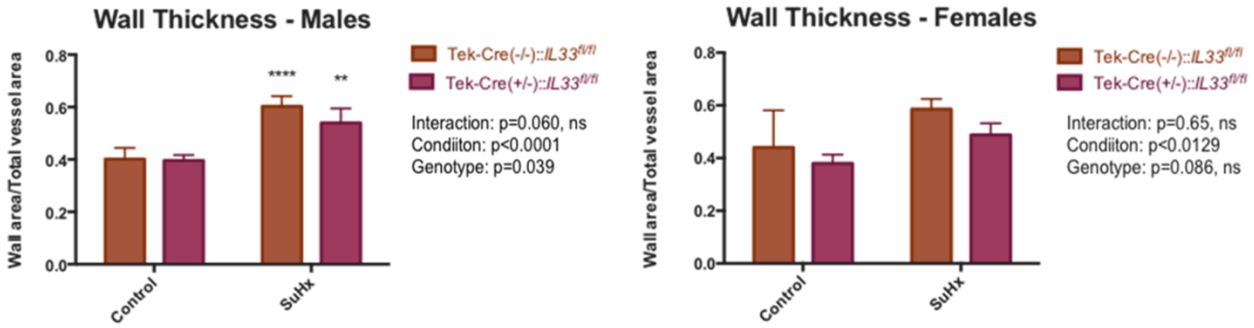

Figure 7: Pulmonary vascular remodeling is not attenuated in Tek-Cre::*IL33*$^{fl/fl}$ male or female mice. * indicates a difference between treatment groups for the same genotype. N = 4

DISCUSSION

The role of IL-33 in pulmonary arterial hypertension: significant findings of our study.

The purpose of our study was to determine whether IL-33 plays a role in the development of pulmonary arterial hypertension through an ST2 or MyD88 pathway. Specifically, we wanted to determine if gene deletion of ST2 or MyD88 prevented the adverse effect on right heart cardiac function that results from the rise in pulmonary vascular resistance due to the inevitable development of pulmonary arterial remodeling characteristic of the disease. We focused on the effect of endothelial cell proliferation, as this cell line has been of particular interest due to its hyperproliferative and antiapoptotic phenotype in patients suffering from advanced forms of the PAH. The significant findings of our study were that both ST2 and MyD88 gene deletion resulted in attenuation of RVP, an effect that was observed across most of the other hemodynamic parameters that we studied in our SuHx-induced murine PAH model. This reduction was also accompanied by a prevention in the thickening of the pulmonary vasculature after chronic SuHx exposure. Whereas ST2 -/- mice, did not demonstrate a protective effect against weight loss, a typical result due to chronic SuHx exposure, they still showed the adverse increase of many parameters that were analyzed to study right heart cardiac function. However, the increases that were observed were still significantly lower than those measured in WT-SuHx mice. In MyD88 -/- mice we did see a protective effect against weight loss after chronic SuHx exposure suggesting that knocking out MyD88 may have the added beneficial effect of preventing the weight loss that is commonly observed in both males and females suffering from PAH. Furthermore, this protective effect due to MyD88 gene deletion was found in all the various hemodynamic parameters that we monitored for all experimental groups to analyze cardiac function including pulmonary vascular remodeling. Altogether, these data suggest that by

knocking out the IL-33 receptor, ST2, and the downstream adaptor protein, MyD88, we can attenuate the progression of PAH.

Inhibition of ST2 or MyD88 expression has a protective effect on right heart cardiac function.

We analyzed various hemodynamic parameters to gain greater insight into cardiac function in the development of PAH, as the right heart is very sensitive to an increase in afterload (Klinger et al., 1991). The right heart can activate mechanisms that allow it to maintain a constant output so that it can adapt to the increased pressures and ejection impedance. These mechanisms often result in changes that lead to RV hypertrophy, followed by RV dilatation. These changes force the right heart to increase its rate of contractility and, once these contractile reserves are exhausted, an irreversible decrease in contractile function develops (Guyton et al., 1954; Bogaard et al., 2009). Thus, by monitoring the instantaneous rates of contractility and relaxation we can learn more about the progression of PAH than by monitoring peak and mean RVP alone. WT-SuHx male mice saw a marked increase in the instantaneous rates of contractility and relaxation. We observed attenuation of these parameters within ST2 -/- and MyD88 -/- males, as none of the changes were significantly different after SuHx exposure when compared to the DMSO/RA control groups. Like the male response, there were significantly elevated levels across all parameters analyzed for cardiac function in WT-SuHx females. However, these were partially attenuated in ST2 -/- females but completely attenuated in MyD88 -/- female mice suggesting a slight difference in response between male and females deficient in the ST2 gene, but with a similar response to a lack of the adaptor MyD88. As both ST2 and MyD88 are key players in the IL-33 signaling pathway, our findings support our hypothesis that IL-33 plays a role in the development of PAH.

Endothelial cell proliferation as a contributing factor to pulmonary arterial hypertension.

Once we gained insight into the role of the IL-33-ST2/MyD88 pathway in PAH development, we then wanted to shift our focus to a possible cellular target. Because endothelial cells have been known to contribute to the progression of pulmonary arterial remodeling, we wanted to quantify these cells in lung tissue to determine if endothelial cells were actively proliferating in our SuHx murine model for PAH. After isolation and enumeration of endothelial cells in lung tissue, we saw more than double the amount of actively proliferating endothelial cells after SuHx exposure. Although not a new finding, our data confirms that our chronic SuHx mouse model for PAH does promote endothelial cell proliferation and supports other studies that have reported similar findings.

Inactivation of *IL33* in endothelial cells does not reduce or prevent the progression of PAH.

As a result of our findings from the endothelial cell enumeration experiment, we further narrowed our focus towards an endothelial cell-specific *IL33* knockout mouse strain in which *IL33* is inactivated in all endothelial cells from birth. The purpose of this study was to determine if *IL3*3 expression specifically by endothelial cells is necessary for the development of PAH. Contrary to our hypothesis, we did not see any reduction in RVP, PA remodeling or in the prevention of weight loss in these mutant mice. Although further studies on this mutant strain are necessary to provide a complete conclusion as to why there was no inhibition in the development of the disease, there are several possible ways to explain these observations: 1. It is possible that we did not inactivate a sufficient portion of the gene. 2. It is also possible that we may be focusing on the wrong cell line, and that a smooth muscle cell-specific *IL33* knockout strain may prove to be more effective at preventing PAH. 3. Much is left to be understood about the mechanism by which IL-33 is released and regulated. Could there be an unknown mechanism

that entirely prevents IL-33 inactivation? Nonetheless, our data are consistent with what other studies that have used this particular *IL33* floxed strain have measured. When Chen *et al.* inactivated *IL33*, an increase in myocardial hypertrophy and overload was also observed (Chen et al., 2015). Could it be that this mouse strain is still allowing IL-33 to activate NF-κB and, thus, is still able to elicit an inflammatory response?

IL33 splice variants and isoforms: possible future targets to gain insight into *IL33* and its role in eliciting an inflammatory response that contributes to disease progression.

To understand the importance of proper inactivation of *IL33*, we must understand the components of the gene itself. The IL-33 gene consists of eight exons. Due to alternative splicing, different IL-33 isoforms are formed from this single gene (Cayrol et al., 2018). Multiple splice variants of IL-33 have been studied with all of their corresponding IL-33 isoforms reported to produce proteins. The most commonly expressed variant is full-length IL-33 (flIL-33), but multiple IL-33 variants are also highly expressed. FlIL-33 has a helix turn helix domain and is localized exclusively to the nucleus (Cayrol et al., 2009); however, extracellular release of flIL-33 may occur when cells undergo necrosis or apoptosis. Furthermore, IL-33 that is released during inflammation is susceptible to post-translational processing which affects its biological activity (Kakkar et al., 2008; Vasanthakumar et al., 2015). For example, flIL-33 is biologically active, and its activity can be enhanced through cleavage by neutrophil serine proteases, cathepsin G and elastase; however, unlike IL-1β, it can be rendered inactive by caspase cleavage (Boitano et al., 2011; Ali et al., 2010). If exon 3 or exon 4 is removed, IL-33 is localized predominantly to the nucleus. Yet, removal of exons 3 and 4 results in IL-33 localization to the nucleus and cytoplasm. Interestingly, any variant that is missing exon 5 will not have cytokine activity, as exon 5 has been shown to be required for IL-33 cytokine activity (Gordon et al.,

2016). More specifically, exon 5 encodes amino acid residues critical for binding of IL-33 to its receptor, transmembrane receptor suppression of tumorigenicity 2 (ST2) (Liu et al., 2013). In our IL33 floxed mouse, exons five through seven were excised. This should have inhibited all cytokine activity caused by IL-33; however, that was not what was observed. It may be possible that other exons that remain may still allow IL-33 to be functional. As mentioned earlier, it may be possible that there is a direct or indirect method by which the first few exons that have not been spliced out can activate NF-κB, which is highly capable of inducing an inflammatory response. Lastly, due to post-translational processing, it is also plausible that the concentration of IL-33 may be affected by tissue integrity and/or environment. It would be interesting to study the effects of these on IL-33 concentration, and thus, regulation and inactivation in greater detail.

The role of smooth muscle cells in PAH.

In addition to endothelial cells, it is also well known that smooth muscle cells proliferate in the pulmonary vasculature as PAH progresses. Perhaps this cell line plays a more critical role than the endothelial cell line, and it could be a focus in a future study. Alternatively, both endothelial cells and smooth muscle cells may be jointly responsible for the vascular remodeling in lung tissue. It has also been proposed that endothelial cells may be transitioning into mesenchymal cells and that this could be the result of the accumulation of smooth muscle-like cells in the occlusive arteriopathy observed in PAH (Arciniegas et al., 2007). The response from Tek-Cre::*IL33*$^{fl/fl}$ mouse line warrants further investigation.

Redox modifications and their effect on IL-33 activity.

Although the regulatory mechanism for IL-33 is not well understood, it has been reported that biological activity of IL-33 at its receptor binding site can be rapidly terminated in the

extracellular environment by the formation of two disulfide bridges (DSB) (Cohen et al., 2005). DSB result in extreme conformational changes that disrupt the ST2 binding site. When IL-33 is present in its reduced form, it remains active. However, if it is oxidized (DSB), it is rendered inactive. Cohen *et al.* explain that this is because mature IL-33 contains four free cysteine residues that are far apart from each other. Thus, cysteine oxidation is a critical regulatory mechanism *in vivo* for rapid termination of IL-33 cytokine activity at its receptor, ST2. Thus, IL-33 oxidation limits the range and duration of immunological responses, and disruption of this mechanism leads to profound enhancement of inflammation. Could it be that there is a mechanism that causes IL-33 to remain in its reduced (active) form within our mouse models? If so, this could further explain as to why inactivation of IL-33 in endothelial cells did not prevent the development of PAH.

IL-33 release mechanism: a continuing enigma.

In vivo studies on mice treated with IL-33 reported pathological changes in pulmonary vasculature, especially in medium and small muscular arteries that developed medial hypertrophy and in which infiltrates of inflammatory cells has been observed (Schmitz et al., 2005). Although IL-33 serves a wide range of functions, including beneficial ones, dependent on tissue type, through its ST2 receptor, it can induce various kinds of inflammatory responses, mainly T_H2- and mast-cell–dependent inflammation. Thus, through studies such as those performed by Schmitz *et al*., we know that IL-33 has an adverse effect on pulmonary vasculature when present at higher concentrations. However, the mechanism by which IL-33 is released is not yet well understood. Some studies have suggested that it is possible that cytoplasmic vesicles are extracellularly transporting it. Although much remains to be confirmed, it has been proposed that these vesicles are released through nuclear pores upon mechanical stress (Kakkar et al.,

2012; Schmitz et al., 2005). Greater understanding of its mechanism of release would further enable it to be used as a target for future therapies involving IL-33.

Limitations of the current mouse model for PAH.

Lastly, the PAH mouse model provides several limitations in the study of this disease, as it does not entirely mimic the pathology observed in humans. Although the search for a suitable mouse model continues, it remains a challenge (Vitali et al., 2014). Yet, the continual advancement in research for this disease remains as crucial as ever. By continuing to pave the way and increase our understanding of the underlying mechanisms that dictate the development of the disease, we should be able to provide new targets for the treatment of pulmonary arterial hypertension.

Summary.

Our studies have highlighted a role of IL-33 in pulmonary arterial hypertension. Although the mechanism by which IL-33 is released remains unknown, and much remains to be understood about how this cytokine is regulated, our results suggest that it warrants further investigation. For now, we have shown that IL-33, through its receptor and downstream adaptor protein MyD88, promotes pulmonary vascular remodeling that leads to the increase of right ventricular pressures. As immunity and vascular inflammation have been deemed a cause rather than a consequence of pulmonary arterial hypertension, our findings support the possibility that the IL-33-ST2/MyD88 pathway is involved in the progression of the disease and may be a target for new therapies. By continuing to study the role of IL-33 in PAH, we may one day provide new hope to this seemingly hopeless population.

REFERENCES

1. Adachi, O., Kawai, T., Takeda, K., Matsumoto, M., Tsutsui, H., Sakagami, M., Nakanishi, K., Akira, S. (1998). Targeted Disruption of the MyD88 Gene Results in Loss of IL-1- and IL-18-Mediated Function. *Immunity, 9*(1), 143-150. doi:10.1016/S1074-7613(00)80596-8.

2. Ali, S., Nguyen, D.Q., Falk, W., Martin, M.U. (2010). Caspase 3 inactivates biologically active full-length interleukin-33 as a classical cytokine but does not prohibit nuclear translocation. *Biochemical and Biophysical Research Communications, 391*(3), 1512-1516. doi:10.1016/j.bbrc.2009.12.107.

3. Arciniegas, E., Frid, M.G., Douglas, I.S., Stenmark, K.R. (2007). Perspectives on endothelial-to-mesenchymal transition: potential contribution to vascular remodeling in chronic pulmonary hypertension. *American Journal of Physiology-Lung Cellular and Molecular Physiology*, *293*(1), L1-L8.

4. Badesch, D.B., Abman, S.H., Simonneau, G., Rubin, L.J., McLaughlin, V.V. (2007). Medical Therapy for Pulmonary Arterial Hypertension: Updated ACCP Evidence-Based Clinical Practice Guidelines. *Chest, 131*(6), 1917-1928. doi:10.1378/chest.06-2674.

5. Barst, R.J., Gibbs, J.S.R., Ghofrani, H.A., Hoeper, M.M., McLaughlin, V.V., Rubin, L.J., Sitbon, O., Tapson, V.F., Galiè, N. (2009). Updated evidence-based treatment algorithm in pulmonary arterial hypertension. *Journal of the American College of Cardiology, 54* (1), S78–84. doi: 10.1016/j.jacc.2009.04.017.

6. Bogaard, H.J., Abe, K., Noordegraaf, A.V., Voelkel, N.F. (2009). The Right Ventricle Under Pressure. *Chest, 135*(3), 794-804. doi: 10.1378/chest.08-0492.

7. Boitano, S., Flynn, A.N., Sherwood, C L., Schulz, S.M., Hoffman, J., Gruzinova, I., Daines, M.O. (2011). Alternaria alternata serine proteases induce lung inflammation and airway epithelial cell activation via PAR2. *American Journal of Physiology. Lung Cellular and Molecular Physiology, 300*(4), L605-L614. doi:10.1152/ajplung.00359.2010.

8. Boraschi, D., Italiani, P., Weil, S., Martin, M.U. (2018). The family of the interleukin-1 receptors. *Immunological Reviews, 281,* 197–232. doi:10.1111/imr.12606.

9. Carriere, V., Roussel, L., Ortega, N., Lacorre, D.A., Americh, L, Aguilar, L., Bouche, G., Girard, J.P. (2007). IL-33, the IL-1-like cytokine ligand for ST2 receptor, is a chromatin-associated nuclear factor in vivo. *Proceedings of the National Academy of Sciences, 104*(1), 282-287. doi:10.1073/pnas.0606854104.

10. Cayrol, C., Girard, J.P. (2009). The IL-1-like cytokine IL-33 is inactivated after maturation by caspase-1. *Proceedings of the National Academy of Sciences of the United States of America, 106*(22), 9021-9026. doi:10.1073/pnas.0812690106

11. Cayrol, C., Girard J.P. (2018). Interleukin-33 (IL-33): A nuclear cytokine from the IL-1 family. *Immunolical Reviews, 281*, 154–168. doi:10.1111/imr.12619.

12. Chalubinski, M., Wojdan, K., Luczak, E., Gorzelak, P., Borowiec, M., Gajewski, A., Rudnicka, K., Chmiela, M., Broncel, M. (2015). IL-33 and IL-4 impair barrier functions of human vascular endothelium via different mechanisms. *Vascular Pharmacology, 73*, 57-63. doi:10.1016/j.vph.2015.07.012.

13. Chen, W.Y., Hong, J., Gannon, J., Kakkar, R., Lee, R.T. (2015). Myocardial pressure overload induces systemic inflammation through endothelial cell IL-33. *Proceedings of the National Academy of Sciences of the United States of America*, *112*(23), 7249–7254. doi.org/10.1073/pnas.1424236112.

14. Choi, Y.S., Choi, H.J., Min, J.K., Pyun, B.J., Maeng, Y.S., Park, H., Kim, J., Kim, Y.M., Kwon, Y.G. (2009). Interleukin-33 induces angiogenesis and vascular permeability through ST2/TRAF6-mediated endothelial nitric oxide production. *Blood, 114*(14), 3117-3126. doi:10.1182/blood-2009-02-203372

15. Ciuclan, L., Bonneau, O., Hussey, M., Duggan, N., Holmes, A.M., Good, R., Stringer, R., Jones, P., Morrell, N.W., Jarai, G., Walker, C., Westwick, J., Thomas, M. (2011). A novel murine model of severe pulmonary arterial hypertension. *American Journal of Respiratory and Critical Care Medicine, 184*(10), 1171–1182. doi:10.1164/rccm.201103-0412OC.

16. Demerouti, E.A., Manginas, A.N., Athanassopoulos, G.D., Karatasakis, G.T. (2013). Complications Leading to Sudden Cardiac Death in Pulmonary Arterial Hypertension. *Respiratory Care, 58*(7), 1246-1254. doi: 10.4187/respcare.02252.

17. Demyanets, S. Konya, V., Kastl, S.P., Kaun, C., Rauscher, S., Niessner, A., Pentz, R., Pfaffenberger, S., Rychli, K., Lemberger, C.E., Martin, R., Heinemann, A., Huk, I., Gröger, M., Maurer, G., Huber, K., Wojta, J. (2011). Interleukin-33 induces expression of adhesion molecules and inflammatory activation in human endothelial cells and in human atherosclerotic plaques. *Arteriosclerosis, Thrombosis, and Vascular Biology, 31(*9), 2080–2089. doi:10.1161/ATVBAHA.111.231431.

18. Fong, T.A, Shawver, L.K., Sun, L., Tang, C., App, H., Powell, T.J., Kim, Y.H., Schreck, R., Wang, X., Risau, W., Ullrich, A., Hirth, K.P., McMahon, G. (1999). SU5416 Is a Potent and Selective Inhibitor of the Vascular Endothelial Growth Factor Receptor (Flk-1/KDR) that Inhibits Tyrosine Kinase Catalysis, Tumor Vascularization, and Growth of Multiple Tumor Types. *Cancer Research, 59*(1), 99-106.

19. Galiè, N., Torbicki, A., Barst, R., Dartevelle, P., Haworth, S., Higenbottam, T., Olschewski, H., Peacock, A., Pietra, G., Rubin, L.J., Simonneau, G. (2004). Guidelines on diagnosis and treatment of pulmonary arterial hypertension: The Task Force on Diagnosis and Treatment of Pulmonary Arterial Hypertension of the European Society of Cardiology. *European Heart Journal, 25*(24), 2243–2278. doi:10.1016/j.ehj.2004.09.014.

20. Galiè, N., Hoeper, M.M., Humbert, M., Torbicki, A., Vachiery, J.L., Barbera, J.A., Beghetti, M., Corris, P., Gaine, S., Gibbs, J.S., Gomez-Sanchez, M.A., Jondeau, G., Klepetko, W., Opitz, C., Peacock, A., Rubin, L., Zellweger, M., Simonneau, G. (2009). Guidelines for the diagnosis and treatment of pulmonary hypertension: The Task Force for the Diagnosis and Treatment of Pulmonary Hypertension of the European Society of Cardiology (ESC) and the European Respiratory Society (ERS), endorsed by the International Society of Heart and Lung Transplantation (ISHLT). *European Heart Journal, 30*(20), 2493–2537. doi:10.1093/eurheartj/ehp297.

21. Gayle, M.A., Slack, J.L., Bonnert, T.P., Renshaw, B.R., Sonoda, G., Taguchi, T., Testa, J.R., Dower, S.K., Sims, J.E. (1996). Cloning of a Putative Ligand for the T1/ST2 Receptor. *Journal of Biological Chemistry, 271,* 5784-5789. doi: 10.1074/jbc.271.10.5784.

22. Gordon, E.D., Simpson, L.J., Rios, C.L., Ringel, L., Lachowicz-Scroggins, M.E., Peters, M.C., Wesolowska-Andersen, A., Gonzalez, J.R., MacLeod, H.J., Christian, L.S., Yuan, S., Barry, L., Woodruff, P.G., Ansel, K.M., Nocka, K., Seibold, M.A., Fahy, J.V. (2016). Alternative splicing of interleukin-33 and type 2 inflammation in asthma. *Proceedings of the National Academy of Sciences of the United States of America, 113*(31), 8765-8770. doi:10.1073/pnas.1601914113.

23. Guyton, A.C., Lindsey, A.W., Gilluly, J.J. (1954). The Limits of Right Ventricular Compensation Following Acute Increase in Pulmonary Circulatory Resistance. *Circulation Research, 2,* 326-332. doi:10.1161/01.RES.2.4.326.

24. Hoshino, K., Kashiwamura, S., Kuribayashi, K., Kodama, T., Tsujimura, T., Nakanishi, K., Matsuyama, T., Takeda, K., Akira, S. (1999). The Absence of Interleukin 1 Receptor–Related T1/St2 Does Not Affect T Helper Cell Type 2 Development and Its Effector Function. *Journal of Experimental Medicine, 190*(10), 1541-1548.

25. Jafri, S., Ormiston, M.L. (2017). Immune regulation of systemic hypertension, pulmonary arterial hypertension, and preeclampsia: shared disease mechanisms and translational opportunities. *American Journal of Physiology-Regulatory, Integrative and Comparative Physiology, 313*(6), R693-R705. doi: 10.1152/ajpregu.00259.2017.

26. Kakkar, R., Lee, R.T. (2008). The IL-33/ST2 pathway: therapeutic target and novel biomarker. *Nature Reviews Drug Discovery, 7,* 827–840. doi: 10.1038/nrd2660.

27. Kakkar, R., Hei, H., Dobner, S., Lee, R.T. (2012). Interleukin 33 as a Mechanically Responsive Cytokine Secreted by Living Cells. *The Journal of Biological Chemistry, 287,* 6941-6948. doi:10.1074/jbc.M111.298703.

28. Kisanuki, Y.Y., Hammer, R.E., Miyazaki, J., Williams, S.C., Richardson, J.A., Yanagisawa, M. (2001). Tie2-Cre Transgenic Mice: A New Model for Endothelial Cell-Lineage Analysis *in Vivo. Developmental Biology, 230*(2), 230-242. doi: 10.1006/dbio.2000.0106.

29. Klinger, J.R., Hill, N.S. (1991). Right ventricular dysfunction in chronic obstructive pulmonary disease. Evaluation and management. *Chest, 99,* 715-723. doi: 10.1378/chest.99.3.715.

30. Küchler, A.M., Pollheimer, J., Balogh, J., Sponheim, J., Manley, L., Sorensen, D.R., De Angelis, P.M., Scott, H., Haraldsen, G. (2008). Nuclear interleukin-33 is generally expressed in resting endothelium but rapidly lost upon angiogenic or proinflammatory activation. *The American Journal of Pathology, 173(*4), 1229-1242. doi:10.2353/ajpath.2008.080014.

31. Liu, X., Hammel, M., He, Y., Tainer, J.A., Jeng, U., Zhang, L., Wang, S., Wang, X. (2013). Structural insights into the interaction of IL-33 with its receptors. *Proceedings of the National Academy of Sciences of the USA, 110*(37), 14918–14923. doi: 10.1073/pnas.1308651110.

32. Liew, F.Y., Girard, J.P., Turnquist, H.R. (2016). Interleukin-33 in health and disease. *Nature Reviews Immunology, 16,* 676-689. doi:10.1038/nri.2016.95.

33. Liew, F.Y., Pitman, N.I., McInnes, I.B. (2010). Disease-associated functions of IL-33: the new kid in the IL-1 family. *Nature Reviews Immunology, 10,* 103-110. doi: 10.1038/nri2692.

34. Lott, J.M., Sumpter, T.L., Turnquist, H.R. (2015). New dog and new tricks: evolving roles for IL-33 in type 2 immunity. *Journal of Leukocyte Biology, 97,* 1037–1048. doi: 10.1189/jlb.3RI1214-595R

35. Ma, W., Han, W., Greer, P.A., Tuder, R.M., Toque, H.A., Wang, K.K.W., Caldwell, R. W., Su, Y. (2011). Calpain mediates pulmonary vascular remodeling in rodent models of pulmonary hypertension, and its inhibition attenuates pathologic features of disease. *Journal Clinical Investigation, 121*(11), 4548-4566. doi:10.1172/JCI57734.

36. Masri, F.A., Xu, W., Comhair, S.A.A., Asosingh, K., Koo, M., Vasanji, A., Drazba, J., Anand-Apte, B., Erzurum, S.C. (2007). Hyperproliferative apoptosis-resistant endothelial cells in idiopathic pulmonary arterial hypertension. *American Journal of Physiology-Lung Cellular and Molecular Physiology, 293*(3), L548-L554. doi:10.1152/ajplung.00428.2006.

37. Moussion, C., Ortega, N., Girard, J.P. (2008). The IL-1-like cytokine IL-33 is constitutively expressed in the nucleus of endothelial cells and epithelial cells in vivo: a novel 'alarmin'? *PLOS ONE, 3*(10), e3331. doi:10.1371/journal.pone.0003331.

38. O'Neill, L.A.J., Bowie, A. G. (2007). The family of five: TIR-domain-containing adaptors in Toll-like receptor signaling. *Nature Reviews Immunology, 7*(5), 353-364. doi:10.1038/nri2079.

39. Peacock, A.J., Murphy, N.F., McMurray, J.J.V., Caballero, L., Stewart, S. (2007). An epidemiological study of pulmonary arterial hypertension. *European Respiratory Journal, 30*(1), 104-109. doi:10.1183/09031936.00092306.

40. Pepke-Zaba, J., Higenbottam, T.W., Dinh-Xuan, A.T., Stone, D., Wallwork, J. (1991). Inhaled nitric oxide as a cause of selective pulmonary vasodilatation in pulmonary hypertension. *Lancet, 338*(8776), 1173-1174. doi:10.1016/0140-6736(91)92033-X.

41. Poynter, M.E., Irvin, C.G., Janssen-Heininger, Y.M.W. (2002). Rapid activation of nuclear factor-kB in airway epithelium in a murine model of allergic airway inflammation. *The American Journal of Pathology, 160*(4), 1325-1334. doi: 10.1016/S0002-9440(10)62559-X.

42. Price, A.E., Liang, H.E., Sullivan, B.M., Reinhardt, R.L., Eisley, C.J., Erle, D.J., Locksley, R.M. (2010). Systemically dispersed innate IL-13-expressing cells in type 2 immunity. *Proceedings of the National Academy of Sciences, 107*(25) 11489–11494. doi:10.1073/pnas.1003988107.

43. Rabinovitch, M., Guignabert, C., Humbert, M., Nicolls, M.R. (2014). Inflammation and Immunity in the Pathogenesis of Pulmonary Arterial Hypertension. *Circulation Research. 115,* 165-175. doi:10.1161/CIRCRESAHA.113.301141.

44. Sakao, S., Tatsumi, K., Voelkel, N.F. (2009). Endothelial cells and pulmonary arterial hypertension: apoptosis, proliferation, interaction and transdifferentiation. *Respiratory Research, 10,* 95. doi:10.1186/1465-9921-10-95.

45. Schermuly, R.T., Ghofrani, H.A., Wilkins, M.R., Grimminger, F. (2011). Mechanisms of disease: pulmonary arterial hypertension. *Nature Reviews Cardiology, 8,* 443-455. doi:10.1038/nrcardio.2011.87.

46. Schmitz, J., Owyang, A., Oldham, E., Song, Y., Murphy, E., McClanahan, T.K., Zurawski, G., Moshrefi, M., Qin, J., Li, X., Gorman, D.M., Bazan, J.F., Kastelein, R.A. (2005). IL-33, an interleukin-1-like cytokine that signals via the IL-1 receptor-related protein ST2 and induces T helper type 2-associated cytokines. *Immunity, 23(*5), 479-490. doi: 10.1016/j.immuni.2005.09.015.

47. Schwartz, C., O'Grady, K., Lavelle, E.C., Fallon, P.G. (2016). Interleukin 33: an innate alarm for adaptive responses beyond T_H2 immunity–emerging roles in obesity, intestinal

inflammation, and cancer. *European Journal of Immunology, 46*(5), 1091–1100. doi:10.1002/eji.201545780.

48. Khrystyna Semen, K., Yelisyeyeva, O., Jarocka-Karpowicz, I., Kaminskyy, D., Solovey, L., Skrzydlewska, E., Yavorskyi, O. (2016). Sildenafil reduces signs of oxidative stress in pulmonary arterial hypertension: Evaluation by fatty acid composition, level of hydroxynonenal and heart rate variability. *Redox Biology, 7,* 48-57. doi:10.1016/j.redox.2015.11.009.

49. Simonneau, G., Gatzoulis, M.A., Adatia, I., Celermajer, D., Denton, C., Ghofrani, A., Gomez Sanchez, M.A., Kumar, R.K., Landzberg, M., Machado, R.F., Olschewski, H., Robbins, I.M., Souza, R. (2013). Updated clinical classification of pulmonary hypertension. *Journal of the American College of Cardiology, 62*(25), Supplement, D34–D41. doi:10.1016/j.jacc.2013.10.029.

50. Soon, E., Holmes, A.M., Treacy, C.M., Doughty, N.J., Southgate, L., Machado, R.D., Trembath, R.C., Jennings, S., Barker, L., Nicklin, P., Walker, C., Budd, D.C., Pepke-Zaba, J., Morrell, N.W. (2010). Elevated Levels of Inflammatory Cytokines Predict Survival in Idiopathic and Familial Pulmonary Arterial Hypertension. *Circulation, 122,* 920-927. doi:10.1161/CIRCULATIONAHA.109.933762.

51. Suresh, K., Servinsky, L., Jiang, H., Bigham, Z., Yun, X., Kliment, C., Huetsch, J.C., Damarla, M., Shimoda, L.A. (2018). Reactive oxygen species induced Ca2+ influx via TRPV4 and microvascular endothelial dysfunction in the SU5416/Hypoxia model of pulmonary arterial hypertension. *American Journal of Physiology-Lung Cellular and Molecular Physiology*. doi:10.1152/ajplung.00430.2017.

52. Tamosiuniene, R., Tian, W., Dhillon, G., Wang, L., Sung, Y.K., Gera, L., Patterson, A.J., Agrawal, R., Rabinovitch, M., Ambler, K., Long, C.S., Voelkel, N.F., Nicolls, M.R. (2011). Regulatory T cells limit vascular endothelial injury and prevent pulmonary hypertension. *Circulation Research, 109,* 867–879. doi:10.1161/CIRCRESAHA.110.236927.

53. Townsend, M.J., Fallon, P.G., Matthews, D.J., Jolin, H.E., McKenzie, A.N.J. (2000). T1/St2-Deficient Mice Demonstrate the Importance of T1/St2 in Developing Primary T Helper Cell Type 2 Responses. *Journal of Experimental Medicine, 191*(6), 1069-1076. doi:10.1084/jem.191.6.1069.

54. Tuder, R. M., Groves, B., Badesch, D.B., Voelkel, N.F. (1994). Exuberant endothelial cell growth and elements of inflammation are present in plexiform lesions of pulmonary hypertension. *The American Journal of Pathology, 144*(2), 275–285.

55. Umebashi, K., Tokito, A., Yamamoto, M., Jougasaki, M. (2018). Interleukin-33 induces interleukin-8 expression via JNK/c-Jun/AP-1 pathway in human umbilical vein endothelial cells. *PLOS ONE, 13*(1), e0191659. doi:10.1371/journal.pone.0191659.

56. Vitali, S.H., Hansmann, G., Rose, C., Fernandez-Gonzalez, A., Scheid, A., Mitsialis, S.A., and Kourembanas, S. (2014). The Sugen 5416/Hypoxia Mouse Model of Pulmonary Hypertension Revisited: Long-Term Follow-Up. *Pulmonary Circulation, 4*(4), 619-629. doi:10.1086/678508.

57. Voelkel, N.F., Gomez-Arroyo, J., Abbate, A., Bogaard, H.J., Nicolls, M.R. (2012). Pathobiology of pulmonary arterial hypertension and right ventricular failure. *European Respiratory, 40*(6), 1555-1565. doi: 10.1183/09031936.00046612.

58. Jiang, Z., Georgel, P., Li, C., Choe, J., Crozat, K., Rutschmann, S., Du, X., Bigby, T., Mudd, S., Sovath, S., Wilson, I.A., Olson, A., Beutler, B. (2006). Details of Toll-like receptor:adapter interaction revealed by germ-line mutagenesis. *Proceedings of the National Academy of Sciences, 103*(29), 10961-10966. doi:10.1073/pnas.0603804103.